ANALYTICAL FRACTURE MECHANICS

DAVID J. UNGER

ACADEMIC PRESS

ANALYTICAL FRACTURE MECHANICS

David J. Unger
Department of Mechanical Engineering and
Engineering Mechanics
Michigan Technological University
Houghton, Michigan

ACADEMIC PRESS
San Diego New York Boston London Sydney Tokyo Toronto

This book is printed on acid-free paper. ♾

Academic Press, Inc.
A Division of Harcourt Brace & Company
525 B Street, Suite 1900, San Diego, California 92101-4495

United Kingdom Edition published by
Academic Press Limited
24-28 Oval Road, London NW1 7DX

Library of Congress Cataloging-in-Publication Data

Unger, David J.
Analytical fracture mechanics / by David J. Unger
p. cm.
Includes bibliographical references and index.
ISBN 0-12-709120-3 (acid-free paper)
1. Fracture mechanics. 2. Mechanics, Analytic. I. Title.
TA409.U64 1995
620.1'126--dc20 95-2193
CIP

PRINTED IN THE UNITED STATES OF AMERICA
95 96 97 98 99 00 QW 9 8 7 6 5 4 3 2 1

ANALYTICAL FRACTURE MECHANICS

To my mother and father, Stella and Anthony Unger

Preface

This book is designed to supplement existing textbooks on fracture mechanics with material related to the analytical solution of partial differential equations that pertain to its theory. It concentrates mainly on the near crack-tip region, on which most current research is being focused. Further, it contains a collection of problems that are drawn from recent research in the fields of elastoplastic and environmentally assisted fracture mechanics. In the course of solving these problems, several different solution techniques are demonstrated.

The Introduction presents a systematic development of fracture mechanics theory. It begins with the equations of continuum mechanics and follows with descriptions of general elastic and plastic theory. Subsequent to these general topics, linear elastic fracture mechanics, plastic strip models, and mode III elastoplastic solutions are presented. Following these, failure criteria, slip line theory, and finite element solutions of the mode I problem are discussed. The Introduction provides the necessary background for understanding the subjects covered in the remainder of the book.

In Chapter 1, an initial value problem for the plastic stress function is solved and corresponding displacements of a mode I elastoplastic problem under plane stress loading conditions are obtained. The prescribed elastic–plastic boundary is found by substituting the elastic small-scale-yielding stresses into the Tresca yield condition. If the properties of the governing Monge–Ampere equation (a second-order and nonlinear partial differential equation) are exploited, then it is possible to reduce the problem to a nonlinear, first-order partial differential equation. The plastic stress function is subsequently obtained through the use of differential geometry theory by finding an integral surface that circumscribes the known elastic (Airy) stress function. Unlike in the analogous mode III problem (Hult and McClintock, [HM 56]), whose solution is also pre-

sented, a disequilibrated stress discontinuity is found in the trailing portion of the plastic zone of the mode I problem. This discontinuity indicates that an elastic unloading and a redistibution of stress must occur if equilibrium is to be established. Despite the appearance of the stress discontinuity, this solution might still approximate the plastic stress field ahead of the crack tip, where unloading is likely to be minimal. Currently, there are no other analytical elastoplastic solutions available for mode I problems involving finite-dimensional plastic zones.

In Chapter 2, an elastoplastic solution is obtained for a mode III problem that is related to a transition in plastic zone shape through changes in the eccentricity of the elliptical plastic region. One can recover from this solution, as special cases, the Cherepanov plastic strip solution and the Hult and McClintock small-scale-yielding solution. Also discussed in this chapter, in connection with the transition model, are an equivalent crack length, energy dissipation rate, and fracture assessment diagram. This model has important implications regarding failure curves on the fracture assessment diagram.

Chapter 3 investigates two different mathematical models that are related to environmentally assisted crack growth. The first model is an incremental approach to crack growth, whereas the second model assumes a continuous growth process. Both series and asymptotic expansions are employed in the solution of the equations of the first model for the onset of hydrogen-assisted cracking. Numerical solutions for the secondary and tertiary phases of environmental crack propagation are then examined. In connection with the second model, a modified Stefan problem is proposed and solved for a certain class of transport-controlled stress corrosion cracking problems. Of particular note is the elegant mathematical solution of the moving boundary value problem that is associated with this problem. This solution resolves the seemingly paradoxical situation that external transport of corrodant can lead to uniform rather than decreasing crack growth rates. The decreasing crack growth rates that are predicted by the conventional Stefan problem are not observed experimentally. This explains why this classic moving boundary value problem for diffusion-controlled phenomena has not been applied previously to fracture problems.

In Chapter 4, a Westergaard formulation of the three principal modes of fracture is provided. Exact linear elastic solutions are presented for infinite plates subject to remote tractions. A quantitative comparison between the exact linear elastic solutions and the small-scale-yielding approximations for stresses, displacements, and elastic–plastic boundaries is then given. Chapter 4 is designed to provide insight into the assumptions and limitations of small-scale yielding.

Acknowledgments

The author acknowledges the support of the National Science Foundation (U.S.A.) under Grant MEA-8404065 for the research reported in Chapter 3 on environmental cracking phenomena. Additional support has been provided by the Center for Mechanics of Materials and Instabilities at the Michigan Technological University and the Office of Research and Graduate Studies at the Ohio State University.

Further thanks are given to Pergamon Press Ltd., Headington Hill Hall, Oxford OX3 OBW, UK, for their kind permission to freely adapt text and figures reprinted from Refs. [Ung 90a, Ung 89a, Ung 92a, LU 88, Ung 89b, Ung 90c, UGA 83] in Sections 1.1, 2.1, 2.2, 3.1, 3.2, 3.3, 4.1, and 4.2. Gratitude is also expressed to Kluwer Academic Publishers, Spuiboulevard 50, P.O. Box 17, 3300 AA Dordrecht, The Netherlands, for their permission to incorporate text and figures reprinted from Refs. [Ung 90b, Ung 91, Ung 92b, Ung 93] in Sections 1.2, 2.3, 2.4, and 4.3.

Section 3.1 of this text contains material from an article coauthored with S. L. Lee [LU 88]. Section 3.1 also contains supplementary computations and figures produced jointly with Y. Seo [SU 88] where indicated. The figures and analyses in Chapter 4 (less Section 4.3) were published originally with W. W. Gerberich and E. C. Aifantis as [UGA 83] or by Aifantis and Gerberich in [AG 78] where noted.

Thanks are also given to J. D. McBrayer for his assistance in the production of the color plates.

Special thanks are extended to my former doctoral thesis adviser, E. C. Aifantis, for guidance and for inspiring my love of research.

Lastly, thanks are given to my wife Carolyn for the love and support she has given to me over the years.

Contents

1
On the Continuance of an Analytical Solution across the Elastic–Plastic Boundary of a Mode I Fracture Mechanics Problem

2
Plastic Zone Transitions

Introduction

The purpose of this introduction is to acquaint the reader with some of the fundamental equations and theorems of mechanics that govern elastic and plastic material behavior. Some fundamental problems pertaining to fracture mechanics, along with their associated partial differential equations and solution techniques, will also be discussed.

I.1 EQUATIONS OF CONTINUUM MECHANICS

The term *continuum* in this section's title refers to a body that is continuous at an infinitesimal scale as opposed to a discretized model, i.e., one that is represented by a collection of individual masses with space between them, as in an atomic lattice. Other terms that one commonly encounters in mechanics literature are *homogeneous* and *isotropic*. A homogeneous body is one whose material properties do not change abruptly, as in an aggregate such as concrete, which is composed of cement and gravel. An isotropic body is one whose material properties do not vary with direction, as in wood, whose properties change with the orientation of the grain. We will restrict our discussion to isotropic and homogeneous bodies.

Equilibrium

All of the problems discussed in this text will neglect inertia (i.e., high acceleration) and the effects of body forces (e.g., weight is negligible in comparison to applied forces on the body). Thus the body will be in a state of equilibrium such that the following system of equations are satisfied for

an isotropic, homogeneous body when expressed in a rectangular Cartesian coordinate system (x, y, z):

$$\sigma_{x,x} + \tau_{yx,y} + \tau_{zx,z} = 0 \tag{I.1-1}$$

$$\sigma_{y,y} + \tau_{xy,x} + \tau_{zy,z} = 0 \tag{I.1-2}$$

$$\sigma_{z,z} + \tau_{xz,x} + \tau_{yz,y} = 0 \tag{I.1-3}$$

where σ_i represents a normal stress in the i direction $(i = x, y, z)$, τ_{ij} represents a shear stress in the ij plane $(j = x, y, z)$, and the variables following a comma designate partial differentiation with respect to those variables; e.g.,

$$\sigma_{i,i} \equiv \frac{\partial \sigma_i}{\partial i}, \text{ etc.} \tag{I.1-4}$$

(Note, as in (I1-4), that the commonly used Einstein summation convention for repeated index $(j = i)$ on an arbitrary second-order tensor A_{ij} will not be employed in this text; i.e., $A_{ii} \neq A_{xx} + A_{yy} + A_{zz}$.)

Equilibrium also requires that shear stresses be symmetrical in the absence of a body couple (true in most applications, with the exception of strong magnetic fields); i.e.,

$$\tau_{ij} = \tau_{ji}. \tag{I.1-5}$$

This assumption reduces the number of stresses to be determined in (I.1-1)–(I.1-3) from nine to six.

The actions of individual stresses on a cube of material are shown pictorially in Fig. I.1-1.

On the surface of a body, the stresses produce a force per unit area called traction t_i $(i = x, y, z)$. The components of the traction may be expressed in matrix form as follows:

$$\begin{Bmatrix} t_x \\ t_y \\ t_z \end{Bmatrix} = \begin{bmatrix} \sigma_x & \tau_{xy} & \tau_{xz} \\ \tau_{xy} & \sigma_y & \tau_{yz} \\ \tau_{xz} & \tau_{yz} & \sigma_z \end{bmatrix} \begin{Bmatrix} n_x \\ n_y \\ n_z \end{Bmatrix} \tag{I.1-6}$$

where n_i $(i = x, y, z)$ are the components of an outward normal unit vector of the surface. The directions of the vectors relative to the inclined surface of a tetrahedron are shown in Fig. I.1-2.

The axes of the Cartesian coordinate system can always be rotated at any point of a body such that all shear stresses disappear from the surface

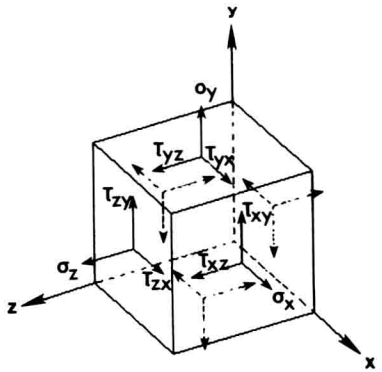

FIGURE I.1-1

Positive stresses acting on various planes of a cube of material in equilibrium.

of the stress cube. The magnitude of stress at this given point is then characterized by three normal stresses ($\sigma_1, \sigma_2, \sigma_3$), which are referred to as the principal stresses.

The magnitude of the maximum shear stress $|\tau_{max}|$ that a body sustains at a point is related to the principal stresses by the formula

$$|\tau_{max}| = \max|\sigma_\alpha - \sigma_\beta|/2, \tag{I.1-7}$$

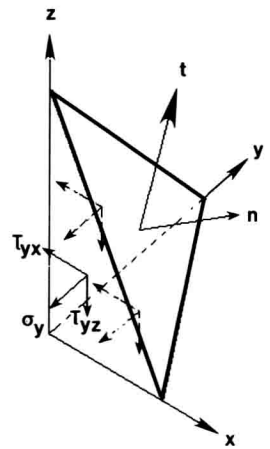

FIGURE I.1-2

Normal and traction vectors on the inclined surface of a tetrahedron.

where $\max|\sigma_\alpha - \sigma_\beta|$ represents the greatest difference between the principal stresses σ_α ($\alpha = 1, 2, 3$) and σ_β ($\beta = 1, 2, 3$).

Strain–Displacement

Small geometric changes of a deforming body are assumed in this text. Consequently, the familiar linearized strain–displacement relationships hold true:

$$\epsilon_x = u_{x,x}, \qquad \epsilon_y = u_{y,y}, \qquad \epsilon_z = u_{z,z} \tag{I.1-8}$$

$$\gamma_{xy} = 2\epsilon_{xy} = u_{x,y} + u_{y,x} \tag{I.1-9}$$

$$\gamma_{xz} = 2\epsilon_{xz} = u_{x,z} + u_{z,x} \tag{I.1-10}$$

$$\gamma_{yz} = 2\varepsilon_{yz} = u_{y,z} + u_{z,y}, \tag{I.1-11}$$

where u_i is the displacement in the i direction, ϵ_i is the normal strain in the i direction, γ_{ij} is the engineering shear strain in the ij plane, and ϵ_{ij} is the shear strain in the ij plane.

Shear strains are symmetrical with respect to the coordinates, i.e.,

$$\gamma_{ij} = \gamma_{ji}, \qquad \epsilon_{ij} = \epsilon_{ji}, \qquad i = x, y, z, j = x, y, z, i \neq j, \tag{I.1-12}$$

as can be seen from their relationships with displacement (I.1-9)–(I.1-11).

Analogous to shear stresses, it is always possible to rotate the orientation of the Cartesian axes at a given point in the body so that all shear strains (I.1-12) vanish. The normal strains that remain at this point in the body after this rotation of axes are called the principal strains ϵ_1, ϵ_2, and ϵ_3, where the subscripts 1, 2, 3 denote the new Cartesian axes.

Change of Volume

The change of volume of a material, ΔV per unit volume of material V, is referred to as the dilatation θ. The dilatation is related to the normal strains as follows:

$$\theta = \Delta V/V = \epsilon_x + \epsilon_y + \epsilon_z = \epsilon_1 + \epsilon_2 + \epsilon_3. \tag{I.1-13}$$

Compatibility of Strains

In general, six equations of strain compatibility must be satisfied in order to obtain a single-valued displacement field. Mathematically, this situation occurs because specifying strain without restriction overdeter-

mines the possible displacement field. These compatibility relationships are

$$\epsilon_{x,yz} = \epsilon_{xy,xz} + \epsilon_{zx,xy} - \epsilon_{yz,xx} \tag{I.1-14}$$

$$\epsilon_{y,xz} = \epsilon_{yx,yz} + \epsilon_{yz,xy} - \epsilon_{zx,yy} \tag{I.1-15}$$

$$\epsilon_{z,xy} = \epsilon_{zx,yz} + \epsilon_{yz,xz} - \epsilon_{xy,zz} \tag{I.1-16}$$

$$\gamma_{xy,xy} = \epsilon_{x,yy} + \epsilon_{y,xx} \tag{I.1-17}$$

$$\gamma_{xz,xz} = \epsilon_{z,xx} + \epsilon_{x,zz} \tag{I.1-18}$$

$$\gamma_{yz,yz} = \epsilon_{y,zz} + \epsilon_{z,yy}. \tag{I.1-19}$$

I.2 EQUATIONS OF ELASTICITY

The following stress–strain relationships hold true for linear elasticity:

$$\sigma_x = \{E/[(1+\nu)(1-2\nu)]\}\big[(1-\nu)\epsilon_x + \nu(\epsilon_y + \epsilon_z)\big] \tag{I.2-1}$$

$$\sigma_y = \{E/[(1+\nu)(1-2\nu)]\}\big[(1-\nu)\epsilon_y + \nu(\epsilon_x + \epsilon_z)\big] \tag{I.2-2}$$

$$\sigma_z = (E/[(1+\nu)(1-2\nu)])\big[(1-\nu)\epsilon_z + \nu(\epsilon_x + \epsilon_y)\big], \tag{I.2-3}$$

where E is Young's modulus and ν is Poisson's ratio (both assumed constant).

Alternatively, we may write strain in terms of stress as

$$\epsilon_x = (1/E)\big[\sigma_x - \nu(\sigma_y + \sigma_z)\big] \tag{I.2-4}$$

$$\epsilon_y = (1/E)\big[\sigma_y - \nu(\sigma_x + \sigma_z)\big] \tag{I.2-5}$$

$$\epsilon_z = (1/E)\big[\sigma_z - \nu(\sigma_x + \sigma_y)\big]. \tag{I.2-6}$$

There are only two independent parameters of linear elasticity for an isotropic material. One alternative parameter, called the shear modulus G, is related to Young's modulus and Poisson's ratio as follows:

$$G = E/[2(1+\nu)]. \tag{I.2-7}$$

This parameter is useful in describing the elastic shear stress and shear strain relationships compactly:

$$\tau_{ij} = G\gamma_{ij}, \qquad i = x, y, z, j = x, y, z, i \neq j. \tag{I.2-8}$$

For an incompressible material Poisson's ratio $\nu = 1/2$.

I.3 EQUATIONS OF PLASTICITY

The two most commonly applied criteria of plastic yield for the modeling of metals are the Mises yield condition and the Tresca yield condition. The Mises yield condition predicts that plastic behavior is initiated in a material when its maximum distortion energy reaches a critical value (see [Men 68]). On the other hand, the Tresca yield condition predicts yield when the maximum shear stress reaches a critical value.

In Cartesian coordinates, the Mises yield condition for incipient plastic flow assumes the form

$$(\sigma_x - \sigma_y)^2 + (\sigma_y - \sigma_z)^2 + (\sigma_z - \sigma_x)^2 + 6\left(\tau_{xy}^2 + \tau_{xz}^2 + \tau_{yz}^2\right) = 2\sigma_0^2, \tag{I.3-1}$$

where σ_0 is the yield stress in simple tension. The relationship between σ_0 and the yield stress in pure shear k for the Mises criterion is

Mises: $$\sigma_0 = 3^{1/2}k \rightarrow k \approx 0.577\sigma_0. \tag{I.3-2}$$

This can be deduced from (I.3-1) by setting all of the stresses equal to zero —save one shear stress, which is given the symbol k.

The Mises yield condition can also be expressed in terms of the three principal stresses (σ_1, σ_2, σ_3) by an equivalent form (4.2-1). One advantage of using (4.2-1) instead of (I.3-2) is that a surface representing (4.2-1) can be visualized in conventional three-dimensional space, with the principal stresses serving as Cartesian coordinates whose base vectors point in the direction of the principal stresses (the Haigh–Westergaard space), whereas (I.3-2) can be visualized only in a generalized sense—as a surface in six-dimensional hyperspace ($\sigma_x, \sigma_y, \sigma_z, \tau_{xy}, \tau_{xz}, \tau_{yz}$).

In the Haigh–Westergaard principal stress space ($\sigma_1, \sigma_2, \sigma_3$), the Mises yield criterion appears as a cylindrical surface of radius $R = (2/3)^{1/2}\sigma_0$ by virtue of a geometric interpretation of Eq. (4.2-1). However, this surface appears as a circle in Fig. I.3-1, as the line of sight is along the central axis; i.e., the generators of the cylinder are perpendicular to the plane of the paper.

In contrast to the Mises yield condition, the Tresca yield condition can be deduced from (I.1-7) as

$$\max|\sigma_\alpha - \sigma_\beta|/2 = k, \qquad \alpha = 1,2,3,\ \beta = 1,2,3, \tag{I.3-3}$$

where k is again defined as the yield stress in pure shear, as it was for the Mises yield condition. Using (I.3-3), by setting all but one of the principal